Cerebral Cortex, January 2020;30: 148–164

doi: 10.1093/cercor/bhz078
Advance Access Publication Date: 30 April 2019
Original Article

ORIGINAL ARTICLE

Dopamine Receptor Expression Among Local and Visual Cortex-Projecting Frontal Eye Field Neurons

Adrienne Mueller, Rebecca M. Krock, Steven Shepard and Tirin Moore

Howard Hughes Medical Institute and Department of Neurobiology, Stanford University School of Medicine, Stanford, CA 94305, USA

Address correspondence to Adrienne Mueller, Department of Neurobiology, Stanford University School of Medicine, Fairchild Bldg, 299 Campus Drive West, Stanford, CA 94305, USA. Email: alm04@stanford.edu.

Abstract

Dopaminergic modulation of prefrontal cortex plays an important role in numerous cognitive processes, including attention. The frontal eye field (FEF) is modulated by dopamine and has an established role in visual attention, yet the underlying circuitry upon which dopamine acts is not known. We compared the expression of D1 and D2 dopamine receptors (D1Rs and D2Rs) across different classes of FEF neurons, including those projecting to dorsal or ventral extrastriate cortex. First, we found that both D1Rs and D2Rs are more prevalent on pyramidal neurons than on several classes of interneurons and are particularly prevalent on putatively long-range projecting pyramidals. Second, higher proportions of pyramidal neurons express D1Rs than D2Rs. Third, overall a higher proportion of inhibitory neurons expresses D2Rs than D1Rs. Fourth, among inhibitory interneurons, a significantly higher proportion of parvalbumin+ neurons expresses D2Rs than D1Rs, and a significantly higher proportion of calbindin+ neurons expresses D1Rs than D2Rs. Finally, compared with D2Rs, virtually all of the neurons with identified projections to both dorsal and ventral extrastriate visual cortex expressed D1Rs. Our results demonstrate that dopamine tends to act directly on the output of the FEF and that dopaminergic modulation of top-down projections to visual cortex is achieved predominately via D1Rs.

Key words: immunofluorescence, macaque, microcircuit, attention, working memory

Introduction

Previous work has established the importance of dopamine signaling in the prefrontal cortex (PFC) for numerous cognitive functions, such as attention and working memory (Williams and Goldman-Rakic 1995; Watanabe et al. 1997; Noudoost and Moore 2011a; Squire et al. 2013; Arnsten 2015). Prefrontal dopamine signaling is thought to play a role in how PFC areas, including the frontal eye field (FEF), sculpt selective attention (Noudoost and Moore 2011b) and may be a target of current medications for attention deficit hyperactivity disorder (Arnsten 2011; Mueller et al. 2017). Dopaminergic input to the macaque PFC stems from several nuclei within the midbrain, including neurons of the substantia nigra and ventral tegmental area (Williams and Goldman-Rakic 1998; Björklund and Dunnett 2007; Bromberg-Martin et al. 2010). Dopamine receptors are classified into two families: D1-like (D1 and D5 receptors) and D2-like (D2, D3, and D4 receptors) (Beaulieu and Gainetdinov 2011). Both receptor subtypes are expressed broadly throughout neocortex, particularly within PFC (Lidow et al. 1989, 1991; Goldman-Rakic et al. 1990). D1Rs and D2Rs tend to have opposing effects on neuronal excitability (reviewed in Seamans and Yang 2004); therefore, differences in the expression of D1Rs and D2Rs across different neuronal classes and layers in the FEF will have profound implications for how dopamine affects the FEF microcircuit.

Early neuropharmacological and neurophysiological experiments provide strong evidence for a role of D1-like, but not D2-like, receptors in working memory-related, persistent activity (Sawaguchi and Goldman-Rakic 1991, 1994;

Williams and Goldman-Rakic 1998). Iontophoretic application of specifically D1-like agonists and antagonists can *both* produce dose-dependent and selective increases or decreases in spiking activity during the memory period of delayed response tasks (Williams and Goldman-Rakic 1995; Vijayraghavan et al. 2007). That is, different doses of D1R agonists or antagonists can selectively enhance persistent activity, but this effect can be caused both by increased spiking for the preferred direction, as well as decreased firing for the non-preferred direction (Vijayraghavan et al. 2007). This observation prompted the hypothesis that D1Rs may mediate the recurrent excitatory interactions thought to underlie persistent activity (Durstewitz et al. 2000; Constantinidis et al. 2001; Wang et al. 2004a), possibly via their influence on glutamatergic synapses (Durstewitz et al. 2000; Gao et al. 2001). Memory-related persistent spiking activity is a common property of neurons within the PFC, including the FEF, an area that is implicated in the control of visual spatial attention (Squire et al. 2013). Infusions of sub-microliter volumes of the D1R antagonist SCH23390 into sites within the FEF increase target selection in the corresponding part of visual space and concomitantly increase the magnitude, stimulus selectivity, and response reliability of visual responses of area V4 neurons with spatially corresponding receptive fields (Noudoost and Moore 2011a). Similar infusions of a D2 agonist result in similar target selection effects, but fail to alter area V4 responses. These results suggest that FEF neurons modulate sensory activity within posterior visual cortex, likely via their direct projections (Stanton et al. 1995; Anderson et al. 2011), and that this influence is shaped by dopamine acting through D1Rs (Noudoost and Moore 2011b). The preponderance of memory-related, persistent activity among FEF neurons projecting to extrastriate cortex (Merrikhi et al. 2017) suggests further that dopamine's effects on persistent activity and on top-down control of visual cortical activity by the FEF occur at the level of layers II-III pyramidal neurons projecting to extrastriate cortex. However, there is no anatomical evidence to support or contradict this possibility.

Previous autoradiographic studies of D1R and D2R expression in macaque dorsolateral PFC showed that D1Rs tend to be expressed across all layers, though most predominantly in layers II, III, and VI, and D2Rs tend to be expressed in deeper layers, most predominantly in layer V (Lidow et al. 1991). Autoradiographic studies, however, lack resolution and may be less specific for individual receptor subtypes. One immunohistochemical study of D1R expression in macaque PFC reported that D1Rs were visible in all cortical areas, but did not quantify the laminar expression patterns (Bergson et al. 1995). In both of these studies, unfortunately, the FEF was not among the areas surveyed. In fact, in spite of the wealth of evidence demonstrating FEF neurons contribute significantly to fundamental components of cognition, no previous work has examined the distribution of dopamine receptors across neuronal classes and cortical layers in this area. We therefore studied the pattern of dopamine receptor expression across different layers and different classes of neurons in the FEF. Additionally, accumulating functional evidence has suggested that D1Rs mediate FEF effects on visual attention, but a paucity of anatomical data has prohibited the development of circuit models to explain these effects. We hypothesized that D1Rs are disproportionately expressed on supragranular FEF neurons that project to extrastriate cortex, and thus we also studied the expression of D1Rs and D2Rs on neurons projecting to dorsal and ventral extrastriate visual cortex.

Materials and Methods

There were two main experiments in this study. The first consisted of staining FEF cortex with neuronal class-specific antibodies as well as dopamine receptor antibodies to identify which neuronal classes express which dopamine receptors and in what proportion. The second involved injecting tracers into posterior visual cortex areas V4 and the middle temporal area (MT), and subsequently staining the FEF for dopamine receptors to identify tracer-labeled neurons in the FEF that project to V4 or MT and express different dopamine receptors. We used three animals for the tracer injections (Monkeys 1, 2, and 3) and tissue from those three animals, as well as three additional animals (4, 5, and 6), for the additional staining studies. Animals were all adult male rhesus macaque monkeys (*Macaca mulatta*). See Table 1 for specific details about the experimental history of the animals used for this study.

Animals were cage-housed and periodically water-restricted for experiments in the time prior to their perfusion. They had daily access to environmental enrichment. Animals also had unlimited access to nutritional biscuits and daily portions of fresh fruit or vegetables. Animals were routinely monitored by animal care, veterinary and laboratory staff and received biannual physicals to establish continued good health. Surgical procedures were under constant supervision by veterinary service personnel, and anesthetic doses and supportive medications were given and adjusted as necessary. Acute illnesses, such as infections, were treated immediately under veterinary guidance. Animals were used for these experiments when they reached the end-of-study time point for other experiments. All experimental procedures were in accordance with the National Institute of Health Guide for the Care and Use of Laboratory Animals, the Society for Neuroscience Guidelines and Policies, and the recommendations of the Stanford University Animal Care and Use Committee. The protocol was approved by the Stanford University Administrative Panel on Laboratory Animal Care.

Tracer Injections

A total of three of the six animals received tracer injections into regions within extrastriate visual cortex. The tracers were purchased from Life Technologies. We used a recombinant version of the cholera toxin B subunit, conjugated with either Alexa Fluor 488, 555, or 594 fluorophores (C22841, C22843, or C22842, respectively). They were mixed with phosphate buffer to a concentration of 1% following the methods of Conte et al. (2009). We injected the left V4 of Monkey 1. For Monkey 2, we performed injections bilaterally into area V4 and into left MT. Monkey 3 received bilateral injections into both V4 and MT. See Table 2 for full details about the injection locations and volumes for these three animals. We only collected tissue from the right hemispheres of Monkeys 2 and 3; therefore, we only list the relevant right hemisphere injections in Table 2. We used two different injection procedures.

Procedure 1: Monkey 1 possessed a recording chamber in which we had previously mapped area V4. We therefore had the chamber coordinates for this region. We performed pressure injections, using a motorized pump (Harvard Pump 11 Plus) to deliver drug from a 100 ul Hamilton glass syringe while the animal was awake. Drug was delivered using a modified injectrode method similar to Noudoost and Moore (2011a), but without the recording probe. Briefly, the tracer was loaded into a Hamilton

Table 1 Animal experimental history

Monkey	Age (years)	Weight (kg)	Experiments	Study-unrelated experiments	Additional health notes
4	12	10.3	Immunofluorescence	Electrophysiological recordings in FEF and V4	None
5	9	9.6	Immunofluorescence	Electrophysiological recordings in V4, pre-perfusion enucleation	None
6	11	12.5	Immunofluorescence	Electrophysiological recordings in FEF and V4, pre-perfusion enucleation	None
1	16	13.5	Tracer, immunofluorescence	Electrophysiological recordings in FEF and V4, pre-perfusion enucleation	Suffered occasional seizures and was chronically medicated with phenobarbital (1.5 mg/kg, 2× daily)
2	4	~5.0	Tracer, immunofluorescence	Pre-perfusion enucleation	None
3	4	~5.0	Tracer, immunofluorescence	Pre-perfusion enucleation	Tested positive for simian retrovirus

syringe that was mounted to a motorized pump and then the syringe was connected to the injectrode via microfluidic components available from LabSmith Inc. The injectrode was then positioned at previously identified V4 coordinates. At each site, we delivered 0.5 µL of tracer at a rate of 1 µL/min at each of 5 depths below the expected pial surface based on measurements taken during previous electrophysiological recordings. We waited 30 s between injections to allow the tracer to disperse.

Procedure 2: Monkeys 2 and 3 did not have recording chambers. They were initially sedated with ketamine (10 mg/kg) and then placed under isofluorane anesthesia (1.0–2.5%). Postoperatively, a combination of buprenorphine and meloxicam analgesia was used. Bilateral craniotomies over visual cortex (see Table 2 for exact sites) were performed under aseptic surgical conditions. A 25 µL Hamilton syringe was held in a UMP3 UltraMicroPump (WPI Inc.) mounted to a stereotaxic arm. The syringe tip was aligned to stereotaxic coordinates for either V4 or MT based on a published macaque brain atlas (Saleem and Logothetis 2012) and injections were made at several sites, and numerous depth locations beneath the cortical surface separated by 0.5 mm (see Table 2). Tracer was injected at a rate of 500 nL/min for 30 s intervals (250 nL per location). We waited 30 s for tracer dispersal before moving to the next location.

For both injection procedures, we cleaned all lines before infusion by passing Nolvasan (Zoetis Services LLC), followed by sterile distilled water and followed by sterile filtered air through the lines. Before being loaded with the tracer and inserted into the brain, the outsides of the injectrode/Hamilton syringe were also cleaned by soaking in Nolvasan, followed by sterile distilled water. For both injection systems, we also verified that the injectrodes/syringes were not clogged by performing brief slow injections and observing formation of a bolus of liquid at the tip of the injectrodes/syringes and by manually inspecting for air bubbles.

Fixation

The monkeys were anesthetized to the surgical plane with isofluorane then initially perfused with 0.25–0.5 L serological saline at high pressure. Animals received 3–4.5% isoflourane and were monitored by veterinary staff prior to and during the perfusion. Animals' corneal and palpebral reflexes were tested (negative) prior to perfusion. We did not apply a lethal injection of pentobarbital, because it can result in a quicker cessation of heartbeat and it is important that the fixative be exposed to tissue that is as healthy and oxygenated as possible for high-quality fixation. The animals were perfused with 4 liters of 3.5–4% paraformaldehyde in 0.1 M phosphate buffer: 2 liters at high pressure over 2–3 min and 2 liters at low pressure over the course of an hour. Finally, they were perfused with 1 liter each of 10%, 20%, and 30% sucrose solutions at high pressure for cryoprotection. Perfusions were performed in the Stanford necropsy suite under ventilation. After perfusion, the brain rested in a 30% sucrose phosphate buffered solution for 7–10 days. We then used a freezing microtome to cut 20 µm coronal sections of the PFC. Slices were stored in phosphate buffered saline (0.1 M) until stained and imaged. Monkeys 2, 4, 5, and 6 had previously been used for electrophysiological experiments, but we did not include tissue that exhibited recording track damage in our analysis.

Immunofluorescence

We co-stained sections with antibodies to D1 or D2 dopamine receptors (αD1R, αD2R), as well as different neuronal markers (see Table 3). We verified the specificity of our antibodies by demonstrating a loss of neuronal immunofluorescence in tissue when the antibodies were absorbed with their specific antigen (see Supplementary Fig. 1A) and the presence of antigen-specific bands of the appropriate size in western blots (see Supplementary Fig. 1B). We used two different D2R antibodies and confirmed there was no significant difference in staining across all layers ($P = 0.1$, 0.97, 0.45, 0.25, and 0.30 for each layer, respectively; see Supplementary Fig. 2). Our working solution for antibody dilutions and washes was 0.1 M phosphate buffer, containing 5% donkey serum (Millipore, S30-100ML) as a blocking agent. For approximately one quarter of our sections, our working solution also contained 0.5% Triton X-100, which is thought to improve permeability. We found no difference in staining when Triton X-100 was included in our working solution and ultimately discontinued its use. Sections were initially washed 3 times then exposed to the working solution (blocking buffer) for 60–90 min. Then the sections were washed 3 times

Table 2 CTB tracer injection locations and volumes

Monkey	Area	Tracer	Number of sites	Number of injections per site	Injection volume	Stereotaxic coordinates—AP	Stereotaxic coordinates—ML	Z-spread—from cortical surface	Total injection volume	Regions exposed to CTB	Volume of injected cortex (mm ^{3})
1	Left V4	CTB-555	8	5 at all	1.25 at all	Locations identified from previous recordings		2–0.5 at all	10 µL	Exclusively V4	3.6
2	Right V4	CTB-488	4	10, 12, 6, 7	2.5, 3, 1.5, 1.75	−5, −3, −2, −1	26, 24.8, 25.5, 27.2	5–0.5, 8–1.5, 6–2.5, 5–1	8.75 µL	Predominantly V4, some V2	7.7
2	Right MT	CTB-555	2	9, 11	2.25, 2.75	−4, −3	20, 20	7–5.5, 14–6	5 µL	Predominantly MT, some area 7a	3.6
3	Right V4	CTB-488	5	8, 12, 9, 7, 4	2, 3, 2.25, 1.75, 1	−5, −4, −3, −2, −2	24, 26, 26, 26, 24	5.5–0, 8–0.5, 6–0.5, 5–0.5, 3–0.5	10 µL	Exclusively V4	38.3
3	Right MT	CTB-555	2	10, 13	2.5, 3.25	−4, −3	19, 20	12–5, 14–6	5.75 µL	Predominantly MT, some MST, some area 7a	60.7

again before being exposed to the primary antibodies at room temperature overnight. The following day the sections were then washed 3 times and exposed to an appropriate secondary antibody for 2 h at room temperature. We used donkey anti-mouse, donkey anti-goat, donkey anti-rabbit, or goat anti-rat Alexafluor antibodies in 488, 568, or 647 wavelengths (ThermoFisher Scientific). The sections were then washed between 6 and 10 times further and exposed to 10 mM cupric sulphate in acetate solution to quench lipofuscin particle fluorescence (Schnell et al. 1999). Finally, the sections were mounted on slides with 4',6-diamidino-2-phenylindole (DAPI)-enriched fluoromount mounting medium (Vector Laboratories, Vectashield, H-1200). DAPI stains DNA and is therefore a label for all nucleated cells.

Imaging

We identified the FEF as the rostral bank of the arcuate sulcus, posterior to the principal sulcus (Moschovakis et al. 2004; Percheron et al. 2015) and performed tile scans of continuous areas of cortex (pial surface to white matter). We imaged sections showing sulcal, para-sulcal, or superficial FEF from either the dorsomedial or ventrolateral banks of the arcuate sulcus. We identified V4 as cortex of the prelunate gyrus, dorsal to the inferior occipital sulcus and between the lunate and superior temporal sulci (Essen and Zeki 1978; Gattass et al. 1988). Sections were imaged with a Leica TCS SP2 AOBS confocal microscope, using a 20× objective and were analyzed using ImageJ. We used estimated optical section thicknesses between 1.8 and 2.5 µm. We collected confocal Z-stacks spanning the 20 µm section depth and collapsed images across the Z-dimension for counting and illustration. Laser power, gain, and offset were optimized at the beginning of an imaging session and not adjusted thereafter. Images were taken using sequential line scans with the different laser wavelengths to reduce bleed-through.

Quantification

We extrapolated the extent of our tracer injections by looking at V4 sections every 240 µm and marking the area of injection spread manually using the software package ImageJ. We could then interpolate between imaged sections to obtain an estimate of the injection spread across those sections. We then approximated the total volume of cortex exposed to the tracer by multiplying the areas by 20 µm, the thickness of our slices, and summing them. See Table 2 for estimates of cortical volume exposed to tracer. We use the scalable brain atlas images to generate the regional outlines for Figure 8 (Dubach and Bowden 2009; Rohlfing et al. 2012).

Our primary assessment was the number of neurons that either 1) were labeled with tracer and also either did or did not express D1Rs or D2Rs or 2) co-expressed a neuronal class marker (e.g. parvalbumin, SMI-32) and either D1Rs or D2Rs. We counted the neurons manually using ImageJ software and the "cell counter" plug-in. We manually counted neurons that expressed either D1R or D2R, as well as a neuronal marker, or both, on each image for each animal. Neurons were identified as being D1R+ or D2R+ if they exhibited fluorescence that was noticeably stronger than the background. For somatically expressed receptors, it is standard to identify them by the presence of strong fluorescent signal that outlines the shape of the full soma (Xu et al. 2003; Noriega et al. 2007; Disney and Reynolds 2014).

Table 3 Antibody information

Antigen	Host	Vendor information	Dilution
D1R	Rabbit polyclonal	ADR-001; Alomone Labs, Jerusalem, Israel	1:200
D2R	Goat polyclonal	SC-7522; Santa Cruz Biotechnology, Santa Cruz, CA	1:200
D2R	Rabbit polyclonal	ADR-002; Alomone Labs, Jerusalem, Israel	1:200
Neurogranin	Mouse monoclonal	SC-514922; Santa Cruz Biotechnology, Santa Cruz, CA	1:200
SMI-32	Mouse monoclonal	NE1023; Millipore, Temecula, CA	1:1000
Parvalbumin	Mouse monoclonal	P3088; Sigma-Aldrich Inc., St. Lous, MO	1:1000
Calbindin	Mouse monoclonal	CB300; Swant Inc., Switzerland	1:1000
Calretinin	Mouse monoclonal	6B3; Swant Inc., Switzerland	1:1000
Somatostatin	Rat monoclonal	MAB354; Millipore, Temecula, CA	1:400

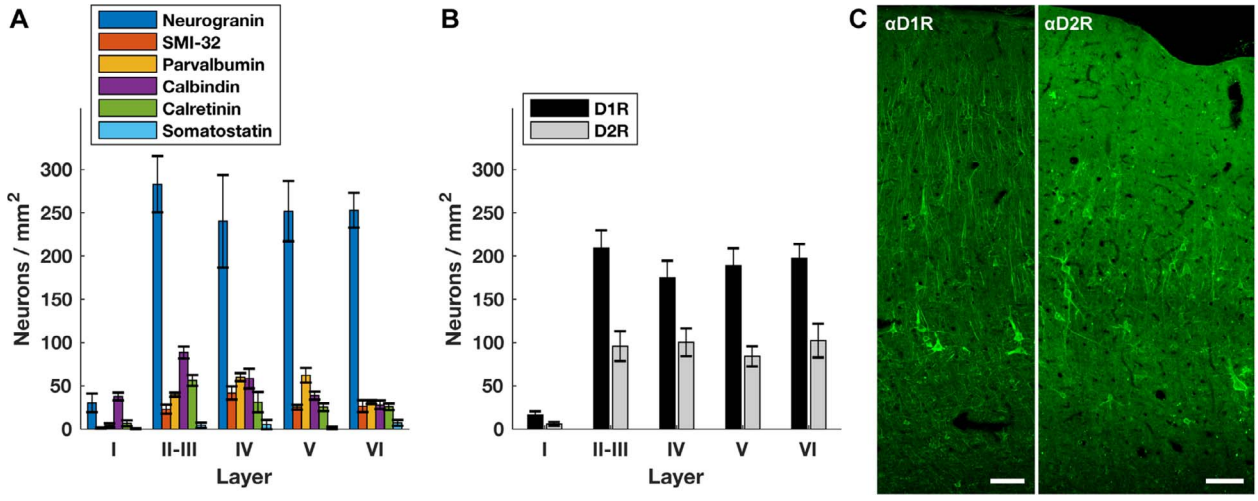

Figure 1. Proportion of neurons expressing dopamine receptors across cortical layers. (*A*) The density of different neuronal classes across cortical layers. (*B*) The density of neurons expressing D1Rs or D2Rs for each cortical layer. (*C*) D1R and D2R expression across FEF cortex. Tissue is from the same animal (Monkey 4) and is oriented with the pial surface at the top and white matter at the bottom. Scale bar = 100 µm.

Although cortical neurons are ~5–20 µm in diameter and rarely are physically abutting, it is theoretically possible that collapsing across the Z-dimension could hide neurons that are completely overlapping along the Z-axis. Our counts are therefore only estimates of the proportion of neurons within an area that expresses a given marker. For some estimates, counts were pooled to generate a measure of the proportion of inhibitory neurons in general. We then averaged counts across all animals. In some cases, we quantified expression for multiple sections for a single animal. In these circumstances, we first averaged within-animal counts before averaging across animals. Proportions for co-expression were calculated from these across-animal averages. We estimated the number of neurons expressing a particular dopamine receptor, neuronal marker, or both across cortex by identifying their positions along the pia/white matter axis. We identified the different cortical layers by visual inspection as follows: Layer I was identified as a region with very few cell bodies. Layer IV, which exists as a very narrow strip in macaque FEF (Huerta et al. 1986; Moschovakis et al. 2004; Percheron et al. 2015), was identified as a thin band with very small, tightly packed cells. Layers II-III were therefore the region in between layers I and IV. Layer V was identified by the presence of large neurons with pyramidal cell morphology. Layer VI was therefore the region between layer V and the predominantly neuron-free white matter.

We made statistical comparisons of frequencies between groups using chi-squared tests and corrected for multiple comparisons using the Bonferroni method. The majority of comparisons were 2 by 2: dopamine receptor presence and absence on two different neuronal classes, resulting in a degree of freedom of 1. In the case of across-layer comparisons for a single neuronal class, there were 3 degrees of freedom. In some cases, we wanted to compare the difference between proportions (i.e. the difference in the D1R proportion compared with the D2R proportion in neurogranin+ neurons compared with the difference in D1R and D2R proportions in extrastriate-projecting neurons). To accomplish this, we used two complementary approaches: a general linear model (GLM) (Agresti 2003) to assess a 3-factor interaction and a bootstrapping method. For the GLM, we used receptor presence (yes or no), receptor type (D1R or D2R), and neuronal class (e.g. neurogranin+ or extrastriate-projecting) as factors. A GLM allows one to express the prediction that the difference in receptor presence and absence between the two receptor types (D1R or D2R) is not the same for one cell type compared with another (Agresti 2003). This relationship is defined by the 3-way interaction term in the model $\mu_{ijk} = \beta_0 + \beta_{\text{Presence}} + \beta_{\text{ReceptorType}} + \beta_{\text{CellType}} + \beta_{\text{Presence ReceptorType}} + \beta_{\text{ReceptorType CellType}} + \beta_{\text{Presence CellType}} + \beta_{\text{Presence ReceptorType CellType}}$, where i, j, and k are indices for the counts for presence/absence, receptor type, and cell type. Then we compared

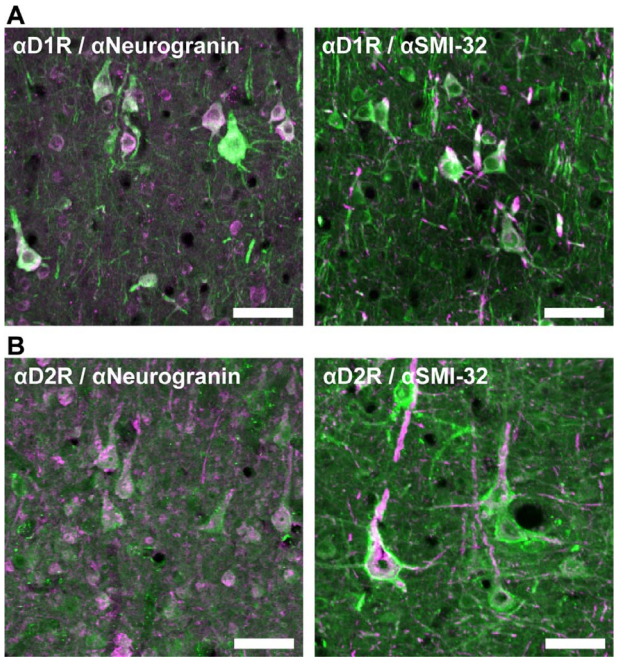

Figure 2. Immunofluorescent staining of dopamine receptors on neurogranin+ and SMI-32+ pyramidal neurons. (*A*) Left: many neurogranin+ pyramidal neurons (pink) express D1Rs (green). Right: the majority of SMI-32+ neurons (pink) also express D1Rs (green). (*B*) Left: several neurogranin+ pyramidal neurons (pink) express D2Rs (green). Right: the majority of SMI-32+ pyramidal neurons (pink) express D2Rs (green). Scale bar = 100 μm.

models with and without the 3-way interaction with neuronal class and used the residual deviances to calculate the *P*-value using a chi-square statistic to determine whether significant variance was explained without the 3-factor interaction or not. In addition, we used a bootstrap method to corroborate the GLM comparisons of differences between proportions. We resampled the proportions of D1R+ and D2R+ neurons for the compared neuronal populations. We resampled each of the compared populations 10 000× and then calculated the probability of observing the ratio of D1R+ expression to D2R+ expression (%D1R+:%D2R) in one population (e.g. extrastriate-projecting) in a different population (e.g. SMI-32+).

Results

We stained FEF sections for two pyramidal neuron markers and four inhibitory neuron markers, as well as for D1 and D2 receptors. Pyramidal neurons were labeled with neurogranin, a more general pyramidal neuron marker (Higo et al. 2004; Singec et al. 2004), or SMI-32, a putative marker for a subset of long-distance projection neurons (Voelker et al. 2004). Interneurons were labeled with markers for independent inhibitory neuron populations, specifically parvalbumin, calbindin, calretinin, and somatostatin. As expected, the density of neurogranin+ pyramidal neurons was several fold greater than that of interneurons across layers II–VI, the greatest difference occurring in layer VI (Fig. 1*A*). As with previous studies in macaque PFC, we also found that the density of parvalbumin+ interneurons peaked in the intermediate layers, whereas calbindin+ and calretinin+ interneurons peaked in superficial layers (Condé et al. 1994). Across all layers, the density of D1 receptor-expressing cell bodies was more than twice that of D2 receptors (Fig. 1*B*, 1*C*).

D1R Expression Is Higher Than D2R Expression among Pyramidal Neurons

We compared the prevalence of D1 and D2 receptors on neurogranin+ and SMI-32+ pyramidal neurons. Neurons labeled by either marker robustly expressed D1Rs and D2Rs (Fig. 2). We found that a higher proportion of pyramidal neurons, both neurogranin+ and SMI-32+, expresses D1Rs than express D2Rs. The majority of neurogranin+ neurons (76.9%) expressed D1Rs, whereas proportionately fewer (51.3%) expressed D2Rs ($P < 10^{-10}$) (Fig. 3). Among the subpopulation of putative long-range projecting SMI-32+ pyramidals, we observed that virtually all neurons (99.3%) expressed D1Rs, whereas a significantly lower proportion (83.7%) expressed D2Rs ($P = 3.2 \times 10^{-13}$).

D1R and D2R Expression among Pyramidal Neurons Changes with Cortical Depth

We compared the proportion of neurogranin+ and SMI-32+ pyramidal neurons expressing D1Rs and D2Rs for each cortical layer. Across layers, the ratio of D1R-to-D2R expression on neurogranin+ pyramidal neurons decreased with cortical depth from ~2 in layers II-III to near unity in layer VI (Fig. 4A; Table 4). There were very few neurogranin+ neurons in layer I, so this layer was excluded from our analyses. We also found that a higher proportion of neurogranin+ neurons expressed D1Rs than D2Rs across all layers, consistent with data shown in Figure 3. This difference was significant in layers II-III ($P < 10^{-10}$), IV ($P = 0.004$), and V ($P = 2.8 \times 10^{-4}$), but not layer VI ($P = 0.03$) (Fig. 4A). Within the two classes of dopamine receptors, expression was largely uniform across layers, with only two significant pairwise differences observed between layers (Table 5).

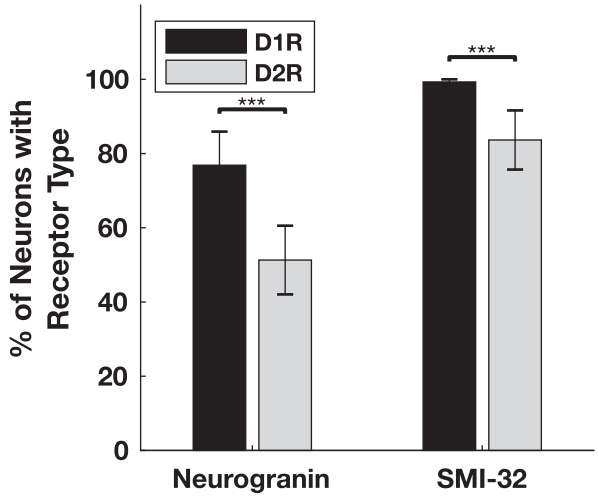

Figure 3. Proportion of neurogranin+ and SMI-32+ pyramidal neurons that express D1Rs or D2Rs. Significantly more neurogranin+ neurons and SMI-32+ neurons express D1Rs (black) than D2Rs (gray). *** denotes significance at the level of 0.001 after Bonferroni correction. Significance was determined using chi-squared tests calculated on total counts (Neurogranin+ $N = 3028$, $P < 10^{-10}$; SMI32+ $N = 225$, $P = 3.2 \times 10^{-13}$). Bar heights and standard error bars are calculated from the across-animal mean proportions, and the exact values are described in the main text. Animal Ns respectively for Neurogranin+ D1R, D2R = 4, 4; SMI-32+ D1R, D2R = 3, 4.

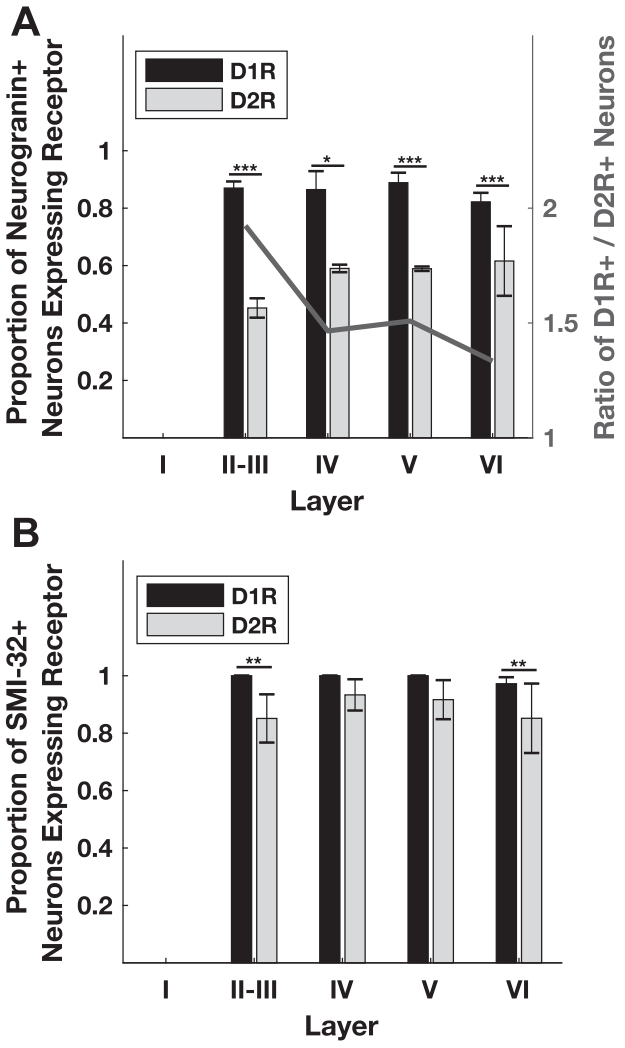

Figure 4. Distribution of dopamine receptors in pyramidal neuron populations across cortical layers. (*A*) The proportion of D1R-expressing neurogranin+ pyramidal neurons is larger than the proportion of D2R-expressing neurogranin+ neurons across all layers. This difference was statistically significant in layers II–V. Overall, the ratio of D1Rs to D2Rs decreases across cortical layers (right *y*-axis). (*B*) The proportion of D1R-expressing SMI-32+ pyramidal neurons is also larger than the proportion of D2R-expressing SMI-32+ neurons across all layers. This difference was statistically significant in layers II-III, and VI. *, **, and *** denote significance at the level of 0.05, 0.01, and 0.001 after Bonferroni correction. Significance was determined using chi-squared tests calculated on total counts. Neurogranin+ $N = 766, 111, 262, 575$; $P < 10^{-16}$, 0.0048, 9.39×10^{-8}, 1.6×10^{-4} for layers II-III, IV, V, and VI, respectively. SMI-32+ $N = 72, 31, 35, 73$; $P = 0.0023$, 0.2, 0.09, and 0.0019 for layers II-III, IV, V, and VI respectively. Bar heights and standard error bars are calculated from the across-animal mean proportions and the exact values are described in Table 4. Animal Ns respectively for Neurogranin+ D1R, D2R = 4, 4; SMI-32+ D1R, D2R = 3, 4.

Specifically, D2Rs were expressed on a significantly higher proportion of neurogranin+ pyramidal neurons in layers V (58.9%, $P = 0.008$) and VI (61.6%, $P = 1.69 \times 10^{-9}$) compared with superficial layers II-III (45.1%).

We found that the overall greater proportion of D1Rs compared with D2Rs among putative long-range projecting SMI-32+ pyramidal neurons (Fig. 3) was not evident in all layers. Instead, the prevalence of D1Rs over D2Rs was only significant in layers II-III ($P = 3.13 \times 10^{-4}$) and VI ($P = 0.001$) (Fig. 4*B*). For both receptor subtypes, expression on SMI-32+ neurons did not significantly vary across layers (Table 5).

Different Classes of Interneurons Express Different Dopamine Receptors

We next compared the prevalence of D1 and D2 receptors on 4 independent classes of inhibitory interneurons: parvalbumin+, calbindin+, calretinin+, and somatostatin+ (Fig. 5). In contrast to pyramidal neurons, we found that overall, a higher proportion of inhibitory neurons express D2Rs (30.5%) than D1Rs (18.9%) ($P < 10^{-16}$; Fig. 6). This difference was primarily attributable to the greater proportion of parvalbumin+ neurons expressing D2Rs (57.8%) compared with D1Rs (16.6%, $P < 10^{-16}$). In contrast, a higher proportion of calbindin+ neurons expressed D1Rs (31.3%) than expressed D2Rs (20.7%, $P = 5.7 \times 10^{-5}$), whereas expression of both receptors was similar for calretinin+ (D1R = 15.4%, D2R = 16.7%, $P = 0.42$) and somatostatin+ (D1R = 31.9%, D2R = 36.1%) neurons. We did not perform a statistical comparison of somatostatin+ neurons because they were so sparsely found in macaque FEF (~3/mm^2).

D1R and D2R Expression among Inhibitory Interneurons Differs across Layers

Finally, we examined the D1R and D2R expression in each inhibitory interneuron class across cortical layers. When examining individual layers, the only significant difference between D1R and D2R expression was among parvalbumin+ neurons (Fig. 7; Table 4), and this difference was evident across layers II–VI. There were no pairwise differences in D1R expression between layers (Table 5); however, there was a significantly higher proportion of D2R-expressing parvalbumin+ neurons in layers V and VI compared with layers II-III (Table 5). Among calbindin+ and calretinin+ neurons, there were no differences in the relative proportion of neurons expressing D1Rs compared with D2Rs in individual layers. However, unlike parvalbumin+ neurons, there were pairwise differences in D1R expression, and not D2R+ expression, between layers among both calbindin+ and calretinin+ neurons (Table 5). In summary, across all layers, the proportion of D2R-expressing parvalbumin+ neurons was always significantly greater than D1R-expressing neurons, and further a significantly higher proportion of parvalbumin+ neurons express D2Rs in deeper layers (V and VI) compared with layers II-III. Also, there are specific differences in D1R expression across different layers among calbindin+ and calretinin+ neurons, but not D2R expression.

Extrastriate-Projecting FEF Neurons Express D1Rs More Than D2Rs

Having examined the expression of dopamine receptors among different classes of FEF neurons, we next examined that expression within the subset of FEF neurons with identified projections to visual cortex. The FEF projects to all areas within posterior visual cortex excluding primary visual (striate) cortex (Schall et al. 1995). Our goal was to examine D1R and D2R expression on FEF neurons with projections to either dorsal or ventral portions of extrastriate visual cortex. To accomplish this, we injected visual cortical areas V4 and MT with cholera-toxin B

Table 4 Proportion of neurons expressing D1Rs or D2Rs across cortical layers: average ± standard error

D1R					
	I	II-III	IV	V	VI
Neurogranin	—	0.87 ± 0.02	0.86 ± 0.06	0.89 ± 0.03	0.82 ± 0.03
SMI-32	—	1.00 ± 0.00	1.00 ± 0.00	1.00 ± 0.00	0.97 ± 0.02
Parvalbumin	—	0.13 ± 0.00	0.18 ± 0.03	0.05 ± 0.04	0.09 ± 0.06
Calbindin	0.06 ± 0.05	0.31 ± 0.03	0.56 ± 0.08	0.36 ± 0.05	0.20 ± 0.03
Calretinin	0.40 ± 0.18	0.12 ± 0.06	0.07 ± 0.04	0.13 ± 0.07	0.37 ± 0.10
D2R					
	I	II-III	IV	V	VI
Neurogranin	—	0.45 ± 0.03	0.59 ± 0.01	0.59 ± 0.01	0.62 ± 0.12
SMI-32	—	0.85 ± 0.08	0.93 ± 0.05	0.92 ± 0.07	0.85 ± 0.12
Parvalbumin	—	0.49 ± 0.16	0.86 ± 0.12	0.74 ± 0.11	0.78 ± 0.03
Calbindin	—	0.23 ± 0.05	0.33 ± 0.14	0.34 ± 0.13	0.24 ± 0.10
Calretinin	0.10 ± 0.07	0.12 ± 0.09	0.00 ± 0.00	0.10 ± 0.07	0.23 ± 0.08

Table 5 *P*-values of layer-versus-layer pairwise comparisons for D1R and D2R expression on different neuronal classes

D1R						
	II-III versus IV	II-III versus V	II-III versus VI	IV versus V	IV versus VI	V versus VI
Neurogranin	0.627	0.719	0.122	0.509	0.762	0.158
SMI-32	—[a]	—	0.255	—	0.350	0.321
Parvalbumin	0.545	0.159	0.882	0.080	0.512	0.236
Calbindin	0.027	0.626	0.288	0.210	**0.008**[b]	0.232
Calretinin	0.602	0.108	**1.5** $^{-4}$[b]	0.176	0.013	0.140
D2R						
	II-III versus IV	II-III versus V	II-III versus VI	IV versus V	IV versus VI	V versus VI
Neurogranin	0.033	**0.008**[b]	**1.7** $^{-9}$[b]	0.888	0.171	0.043
SMI-32	0.215	0.351	0.567	0.681	0.119	0.190
Parvalbumin	0.017	**0.008**[b]	**0.002**[b]	0.479	0.880	0.466
Calbindin	0.687	0.966	0.572	0.739	0.944	0.699
Calretinin	0.265	0.520	0.978	0.433	0.277	0.581

[a]Performance of a chi-squared or Fisher's exact test was not valid in the case of these comparisons, because for several layers the frequency of SMI-32+ neurons without D1R expression was zero.
[b]Bolded values are significant at Bonferroni-corrected p-value thresholds equivalent to $P < 0.05$.

tracers conjugated to different colors of fluorophores (Fig. 8). A total of 8, 4, and 5 injections were made within area V4 (Monkeys 1, 2, and 3, respectively; Table 2). Injections were placed into cortex on the surface of the prelunate gyrus where prior electrophysiological recordings were carried out in one animal (Monkey 2), and where the lower central visual field is represented (Gattass et al. 1988). Another two injections (Monkeys 2 and 3, respectively) targeted area MT and were placed into cortex near the caudal floor of the superior temporal sulcus (STS) (Table 2). The location of injection sites primarily within the floor and lower bank of the STS suggests that they covered more central visual field locations (Gattass and Gross 1981). However, the precise placement of the injections within the visual field map in MT was not specifically determined. The sites shown in Figure 8 depict the center of the injections, where the injection volume was largest and therefore demonstrate the maximum amount of spread. In the MT injections, some tracer spread was observed in nearby areas, such as 7a and MST. Overall, the injections were largely confined to the target areas, particularly in area V4.

We next identified labeled neurons within the FEF (Fig. 9) and compared the relative expression of the two classes of dopamine receptors. As expected, retrogradely labeled pyramidal neurons from the two extrastriate injections were found predominantly in layers II-III. Both D1 and D2 receptors were expressed on FEF projection neurons (Fig. 10). However, we observed that the proportions of D1R and D2R-expressing projection neurons were different (Fig. 11). Whereas 91.8% of the total population of projection neurons expressed D1Rs, only 46.5% of them expressed D2Rs (Fig. 11A), a difference that is significant ($P < 10^{-16}$). The disproportionate expression was also significant in both of the subpopulations of dorsal (MT-projecting) ($P < 10^{-16}$) and ventral (V4-projecting) ($P = 5 \times 10^{-4}$) projecting neurons (Fig. 11B). In addition, this difference in receptor expression among extrastriate-projecting neurons was significantly greater than the difference observed among the SMI-32+ ($P < 10^{-16}$) and the neurogranin+ ($P < 10^{-16}$) neuron populations (see Supplementary Fig. 3). Thus, the predominance of D1R expression among pyramidal neurons was particularly strong for neurons projecting to extrastriate visual cortex.

Discussion

This is the first systematic examination of D1R and D2R expression on different neuronal classes in the macaque FEF. We found that dopamine receptors in the FEF are more prevalent on

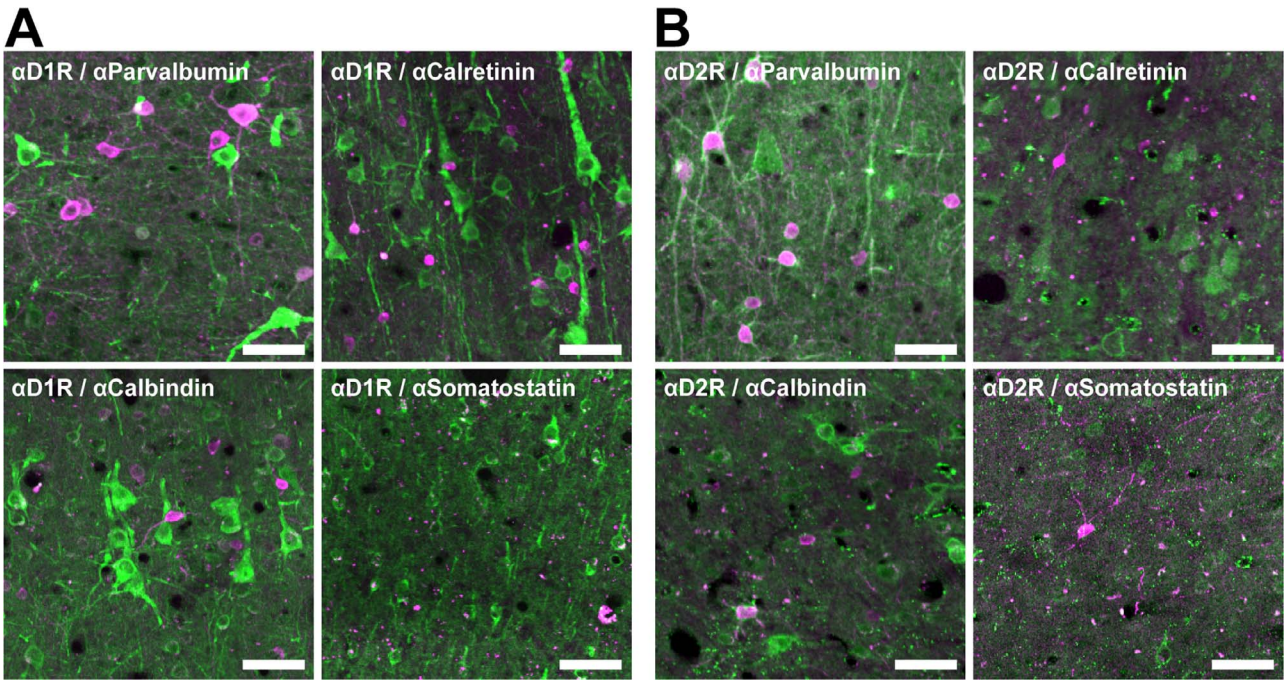

Figure 5. Immunofluorescent staining of dopamine receptors on inhibitory interneuron classes. (*A*) Inhibitory interneuron classes (pink) rarely express D1Rs (green). (*B*) Parvalbumin+ interneurons (pink) frequently express D2Rs (green), but other inhibitory neuron classes (pink) do not. Scale bar = 50 μm.

pyramidal neurons than on inhibitory interneurons, and that among pyramidal neurons a higher proportion of both neurogranin+ and SMI-32+ neurons express D1Rs than express D2Rs. The ratio of D1R-to-D2R expression on neurogranin+ pyramidal neurons decreased with cortical depth from ~2 in layers II-III to near unity in layer VI. There were also neuron class-specific differences in dopamine receptor expression among inhibitory interneurons; a significantly higher proportion of parvalbumin+ interneurons expressed D2Rs than D1Rs, and vice versa for calbindin+ neurons. Finally, in contrast to D2Rs, virtually all extrastriate-projecting pyramidal neurons expressed D1Rs.

D1Rs Are More Prevalent on Pyramidal Neurons Than Interneurons

We observed a substantially higher rate of expression of D1Rs among pyramidal neurons than among inhibitory interneurons, specifically parvalbumin+, calbindin+, calretinin+, and somatostatin+ interneurons. Particularly for the former three interneuron classes, which were by far the most common and thus for which reliable measurements could be obtained, we observed D1R expression in less than one-third of neurons. In contrast, neurogranin+ or SMI-32+ pyramidals expressed D1Rs at more than twice that rate. Similar to what we observed in the FEF, Bergson et al. (1995) found that D1Rs are prominent on pyramidal neurons in area 46, which neighbors the FEF. This pattern is also similar to the relative expression of D5Rs in the FEF that we recently reported (Mueller et al. 2018). D5Rs, the other member of the D1-like receptor family (Missale et al. 1998), were found to be more prevalent on pyramidal neurons than interneurons, particularly putative long-range projecting (SMI-32+) pyramidal neurons. Thus, we expect that D1/D5 mediated modulation of FEF activity acts primarily through pyramidal neurons.

Differences in D1R and D2R Expression among Pyramidal Neurons

We found that a higher proportion of pyramidal (neurogranin+) neurons overall express D1Rs than D2Rs. However, the difference in proportion was not conserved across cortical layers. In neighboring area 46, Goldman-Rakic et al. (1990) and Smiley et al. (1994) respectively showed higher expression of D1Rs in layers I and II, medium expression in layers V and VI, and lower expression in layers IIIb and IV. Goldman-Rakic et al. (1990) found that D2R expression was strongest in layer V. In the FEF, we found that as cortical depth increased, the ratio of D1R+ neurogranin+ (pyramidal) neurons to D2R+ neurogranin+ neurons decreased. This suggests that a higher proportion of superficial pyramidal neurons, which are more likely to project to visual cortex (Schall et al. 1995; Stanton et al. 1995; Ungerleider et al. 2008), express D1Rs than D2Rs, whereas deep pyramidal neurons, which tend to project to subcortical structures (Parthasarathy et al. 1992; Schnyder et al. 1985), express D1Rs and D2Rs in similar proportions. Indeed, several recent studies have shown that neurons in superficial and deep layers of cortex exhibit distinct electrophysiological features and that correspond to functional differences (Senzai et al. 2019); for example, memory delay activity in macaque PFC was predominantly confined to superficial layers (Bastos et al. 2018). Our result is not only similar to previous reports of dopamine receptor expression in other areas of PFC (Lidow et al. 1991; Bergson et al. 1995), it corroborates the model proposed by Noudoost and Moore (2011b) that hypothesized high proportions of D1Rs on superficial pyramidal

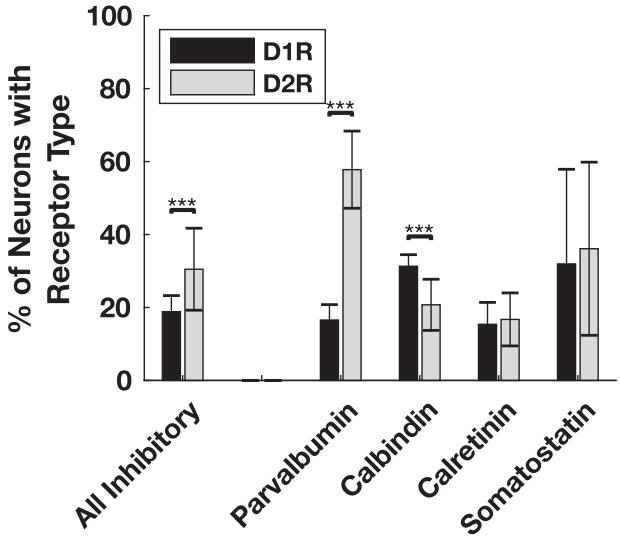

Figure 6. Proportion of inhibitory interneuron classes that express D1Rs or D2Rs. A significantly higher proportion of parvalbumin+ inhibitory interneurons express D2Rs than D1Rs. A significantly higher proportion of calbindin+ inhibitory interneurons express D1Rs compared with D2Rs. When pooling across interneuron classes, the proportion of D2R-expressing interneurons is significantly greater than the proportion of D1R-expressing interneurons. We did not perform a statistical comparison between D1R- and D2R-expressing somatostatin+ neurons because they were so rare. *** denotes significance at the level of 0.001 after Bonferroni correction. Significance was determine using chi-squared tests calculated on total counts (Parvalbumin+ $N = 635$, $P < 10^{-16}$; Calbindin+ $N = 624$, $P = 5.7 \times 10^{-5}$; Calretinin+ $N = 648$, $P = 0.42$). Bar heights and standard error bars are calculated from the across-animal mean proportions and the exact values are described in the main text. Animal Ns respectively for Parvalbumin+ D1R, D2R = 4, 3; Calbindin+ D1R, D2R = 4, 4; Calretinin+ D1R, D2R = 3, 4; Somatostatin+ D1R, D2R = 3, 4.

neurons and a greater prevalence of D2Rs on deep pyramidal neurons.

Different Classes of Interneurons Express Different Dopamine Receptors

We found that D2Rs are disproportionately expressed on parvalbumin+ neurons compared with D1Rs, whereas D1Rs are disproportionately expressed on calbindin+ neurons compared with D2Rs. Parvalbumin+ neurons primarily directly inhibit pyramidal neurons (Williams et al. 1992; Melchitzky et al. 1999), as do calbindin+ neurons, whereas calretinin+ neurons primarily inhibit other inhibitory neurons (DeFelipe 1997). The effects of dopamine on neuronal excitability are very complex (reviewed in Seamans and Yang 2004); however, several studies in rodent and primate PFC have demonstrated D1R activation and D2R activation usually result in opposing effects on neuronal activity: D1R activation frequently increases neuronal excitability (Zheng et al. 1999; Henze et al. 2000; Seamans et al. 2001; Wang and O'Donnell 2001; Gonzalez-Islas and Hablitz 2003), whereas D2R activation usually decreases neuronal excitability (Gulledge and Jaffe 1998; Tseng and O'Donnell 2004, 2007). Although in macaque, it has also been shown that D2R stimulation can increase the activity of some neurons (Wang et al. 2004b; Ott et al. 2014; Vijayraghavan et al. 2016). The differential expression of these receptor types on different neuronal classes should therefore have profound implications for the effect of dopamine on the FEF microcircuit.

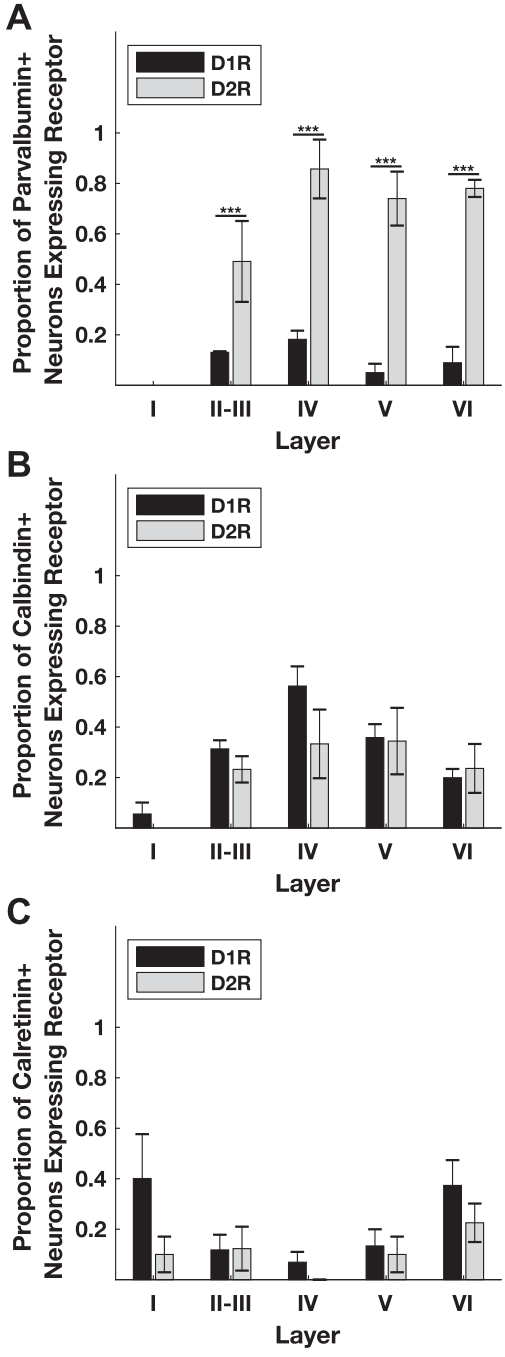

Figure 7. Distribution of dopamine receptors across inhibitory neuron populations across cortical layers. (*A*) Across all layers, the proportion of D2R-expressing parvalbumin+ neurons is higher than the proportion of D1R-expressing parvalbumin+ neurons. (*B*) There is no significant difference in the relative prevalence of D1Rs compared with D2Rs in calbindin+ neurons across layers. (*C*) There is no significant difference in the relative prevalence of D1Rs compared with D2Rs in calretinin+ neurons across layers. Significance was determined using chi-squared tests calculated on total counts. Parvalbumin+ $N = 197, 44, 88, 75$; $P = 1.98 \times 10^{-7}, 3.89 \times 10^{-5}, 1.36 \times 10^{-10}, 4.65 \times 10^{-9}$ for layers II, III, IV, V, and VI, respectively. Calbindin+ $N = 232, 34, 46, 70$; $P = 0.64, 0.46, 0.61, 0.31$ for layers II, III, IV, V, and VI, respectively. Calretinin+ $N = 352, 31, 41, 52$; $P = 5.04 \times 10^{-4}$, 0.42, 0.87, and 0.27 for layers II, III, IV, V, and VI, respectively. Bar heights and standard error bars are calculated from the across-animal mean proportions and the exact values are described in Table 4. Animal Ns respectively for Parvalbumin+ D1R, D2R = 4, 3; Calbindin+ D1R, D2R = 4, 4; Calretinin+ D1R, D2R = 3, 4.

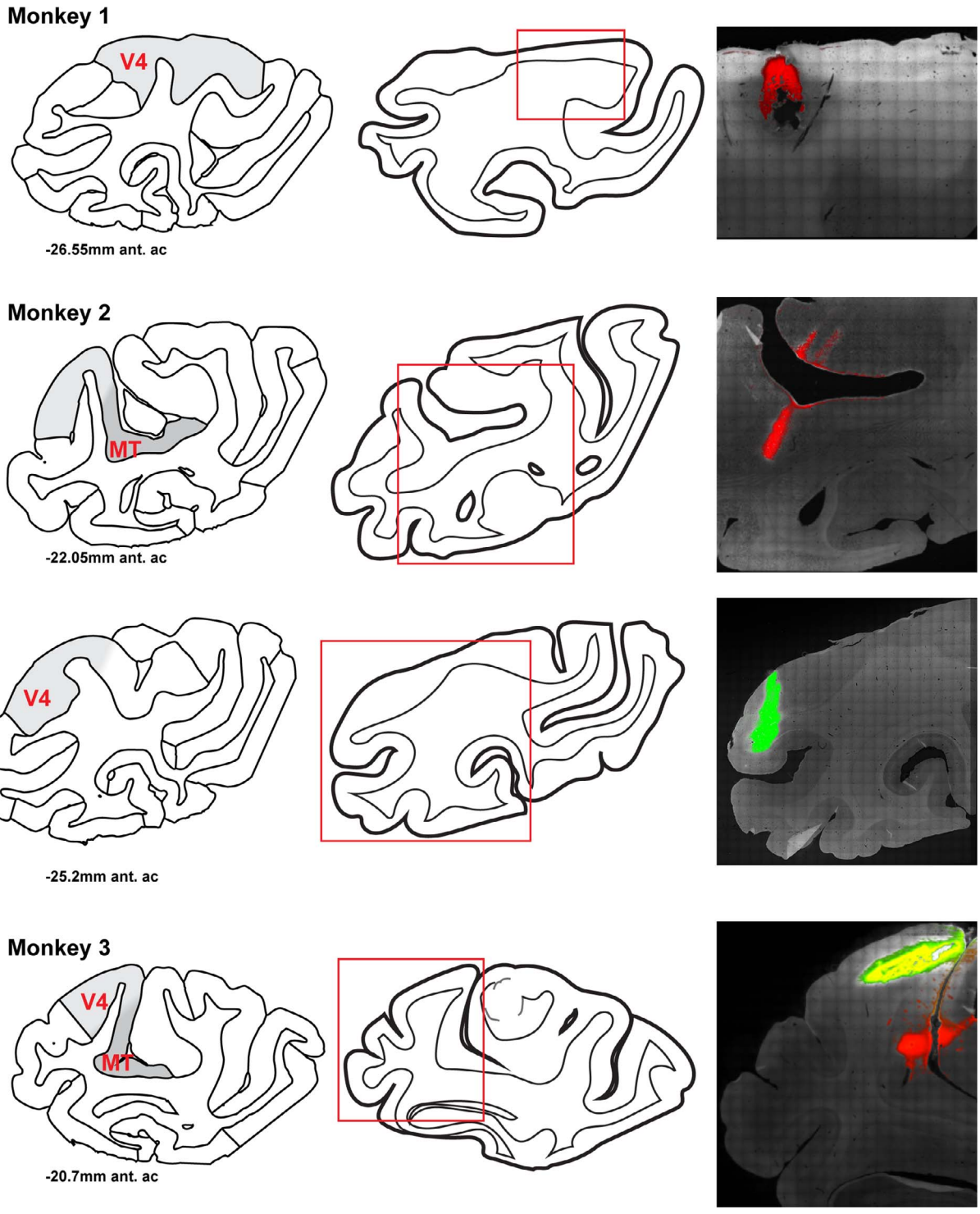

Figure 8. Location of CTB tracer injection sites in three monkeys. For each animal, left is an atlas diagram of the region of cortex close to the center of an injection (Dubach and Bowden 2009; Rohlfing et al. 2012), modified with shading indicating regions MT and V4. The abbreviation 'ant. ac' denotes the relative position of the section anterior to the anterior commissure. Center is a traced outline of the section with the region of the tracer injection visualized in the right panels denoted by a red box. Right is a fluorescent image of the injection site(s). Red is CTB-555, green is CTB-488. Monkey 1 has a CTB-555 injection site in V4. Monkey 2 has a CTB-555 injection site in MT and CTB-488 injection site in V4. Monkey 3 has a CTB-555 injection site in MT and a CTB-488 injection site in V4.

Some interneuron classes within primate area 46 differentially express D1Rs in their processes (Glausier et al. 2009). However, only one recent study has examined the expression of D1Rs on different interneuron populations in the macaque PFC. In area 46, it was found that 98% of parvalbumin+ neurons express D1Rs, 80% of calbindin+ neurons express D1Rs, and

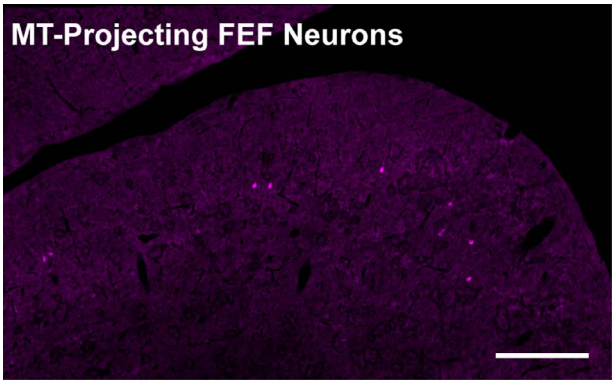

Figure 9. Example of MT-projecting FEF neurons. CTB-555 labeled FEF neurons retrogradely labeled from an MT injection are visible in pink. This section is from the dorsomedial, parasulcal-superficial FEF of Monkey 2. The sulcus is the dorsomedial arcuate. Scale bar = 500 µm.

40% of calretinin+ neurons express D1Rs (Muly et al. 1998). These proportions are very different from what we find in the FEF, where we observed much lower proportions of D1R expression across all classes of interneurons. This difference is most striking for parvalbumin+ FEF neurons, in which we find D1Rs to be expressed in only 16.6% parvalbumin+ neurons. Although some of these differences may reflect differences in labeling techniques (e.g. the use of a quenching agent to suppress lipofuscin particle fluorescence), it is possible that they reflect real differences in the expression of dopamine receptors in area 46 and the FEF. This latter possibility seems compelling given the substantial differences in the functions and connectivity of these two areas and the latter's direct involvement in saccadic control. Nonetheless, future studies should examine the differences in dopamine receptor expression between 46 and the FEF (as well as other PFC areas) in the same tissue.

Dopaminergic Modulation within the FEF Microcircuit

The pattern of dopamine receptor expression we observe across different neuronal classes should inform our understanding of how dopamine influences the activity of FEF neurons. D1R activation of pyramidal neurons in the macaque PFC tends to increase neuronal excitability (Henze et al. 2000; González-Burgos et al. 2002), whereas D2R activation tends to decrease neuronal excitability (Beaulieu and Gainetdinov 2011; although see Wang et al. 2004b; Vijayraghavan et al. 2016). Therefore, dopaminergic input to the FEF may primarily increase the excitability of pyramidal neurons through D1Rs and decrease the excitability of parvalbumin+ interneurons through D2Rs. If true, then the combined effect of dopaminergic input might be an increase in the excitability of pyramidal neurons, both directly through D1Rs and indirectly through D2R-mediated disinhibition via parvalbumin+ neurons, as the primary targets of parvalbumin+ neurons are local pyramidal neurons (Williams et al. 1992; Melchitzky et al. 1999). However, dopamine's action on the PFC is complex and both neuronal responses (Williams and Goldman-Rakic 1995; Sawaguchi 2001; Vijayraghavan et al. 2007) and behavior (Cools and D'Esposito 2011; Fallon et al. 2015) have been shown to exhibit an inverted-U dose–response pattern. For example, D1R activation can also result in a *decrease* in neuronal activity in the PFC of behaving monkeys (Vijayraghavan et al. 2007). Excessive dopaminergic input to the FEF could cause a decrease in pyramidal neuron excitability through several mechanisms. One, high D1R activation decreases the excitability of pyramidal neurons through N-methyl-D-asparte (NMDA) receptor-related cell-intrinsic mechanisms (Wang and O'Donnell, 2001; Gonzalez-Islas and Hablitz 2003; Tseng and O'Donnell 2004). Two, D1R overstimulation may enhance co-localized HCN and KCNQ channel activity causing hyperpolarization of pyramidal neurons (see (Arnsten 2015) for review). A final possibility is that excessive dopamine activates additional, non-parvalbumin+, interneuron classes through volume transmission, ultimately resulting in suppression of pyramidal neuron activity. Future studies are needed to address how dopamine generates these complex responses by examining the effect of dopamine on specific classes of PFC neurons.

Species Differences in Prefrontal Dopamine

The rodent medial prefrontal cortex (mPFC) has often been invoked as a model for the study of human-like cognition (Uylings et al. 2003; Bicks et al. 2015; Tsutsui et al. 2016). Given the apparent importance of prefrontal dopamine for cognition, it is important to consider the similarities and differences between rodent and nonhuman primate species. In addition to several reported differences in dopaminergic innervation of the cerebral cortex and thalamus between rodent and nonhuman primates (Levitt et al. 1984; Berger et al. 1991; García-Cabezas et al. 2009), there are many differences in dopamine receptor expression as well. In the mouse mPFC, D1R+ neurons are mainly found in deep layers, and D2R+ neurons are mainly in superficial layers (Wei et al. 2017). This is opposite to the pattern we observe. *In situ* examinations of expression of D1R and D2R mRNA-containing neurons performed in rat frontal cortex also showed D1R-containing neurons were most abundant in layers V and VI (Gaspar et al. 1995), but, unlike in mouse, D2R mRNA was primarily restricted to layer V as well. At the protein level, immunological studies in rat mPFC also show that the density of D1R+ neurons is almost one-third lower in layers II-III than layers V and VI (Vincent et al. 1993). Furthermore, this study showed a higher density of D2R+ neurons than D1R+ neurons in layers II-III. These latter findings are also opposite to the pattern we found in the macaque. Further, *in situ* studies examining different classes of neurons in the rat mPFC found that D1R expression is lower in pyramidal neurons compared with inhibitory neurons (11–21% vs. 25–52%) and that D2Rs are expressed in only 4–5% of pyramidal neurons and 5–15% of GABAergic neurons (Santana et al. 2009; Santana and Artigas 2017). Not only is the overall dopamine receptor expression much lower in the rat, but also the pattern of D2R and D1R expression is the opposite of what we, and others (Lidow et al. 1991), find in the macaque. Combined, these very divergent results suggest differences in the role of dopamine in primate PFC compared with rodent mPFC.

Extrastriate-Projecting FEF Neurons Are Modulated Predominantly through D1Rs

We found that within the FEF, pyramidal neurons are more likely to express D1Rs or D2Rs than inhibitory neurons. Furthermore, we found that across three different classes of pyramidal

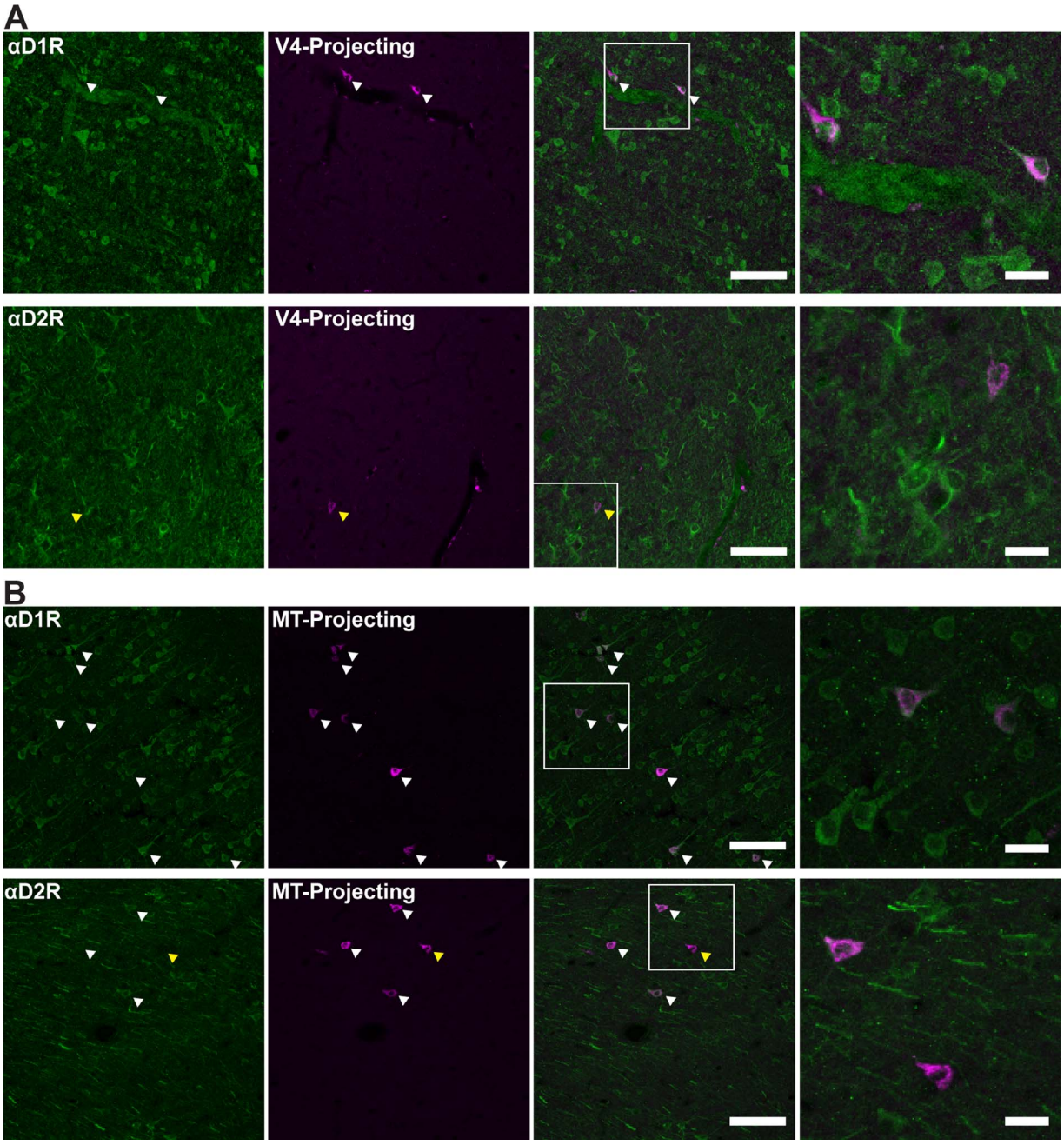

Figure 10. Visual cortex-projecting neurons express dopamine receptors. (A) D1Rs and D2Rs (leftmost, green) presence on V4-projecting FEF neurons (left-center, pink). Overlay image is center-right. The white box indicates the region zoomed in on (rightmost). (*B*) D1Rs and D2Rs (leftmost, green) presence on MT-projecting FEF neurons (left-center, pink). Overlay image is center-right. The white box indicates the region zoomed in on (rightmost). White arrowheads denote co-labeled cells. Yellow arrowhead indicates visual cortex-projecting FEF neurons that do not express D2Rs. Scale bar = 100 μm for leftmost, left-center, and right-center panels, 25 μm for rightmost panel.

neurons (neurogranin+, SMI-32+, and extrastriate-projecting), pyramidals are more likely to express D1Rs than D2Rs. We observed a significantly higher rate of D1R expression than D2R expression among both the dorsal (MT) and ventral (V4) extrastriate-projecting FEF neurons, but particularly among dorsal-projecting FEF neurons. The greater ratio of D1R-to-D2R expression observed in the dorsal-projection population might be due to differences in the placement of tracer within the two targeted extrastriate areas; that is, into nonoverlapping visual field representations. Nonetheless, in the pooled (dorsal and ventral) population of extrastriate-projecting FEF neurons, the difference in proportions of neurons expressing D1Rs and those expressing D2Rs is significantly greater than that observed among the (putative long-range projecting) SMI-32+ neuron populations.

SMI-32 has been shown in some nonhuman primate cortical tissue to disproportionately label neurons in layers V and VI (Campbell and Morrison 1989), which predominantly target

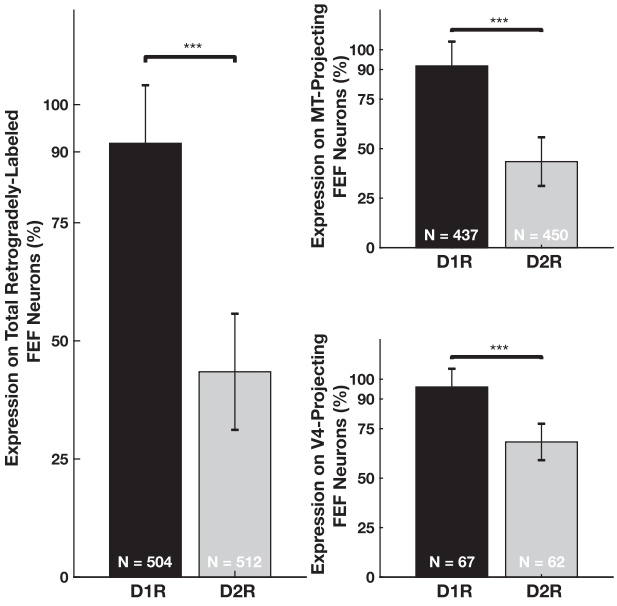

Figure 11. Relative proportion of D1R- and D2R-expressing visual cortex-projecting FEF neurons. The left panel shows the proportion of the 2 populations (V4-projecting and MT-projecting) of neurons that express either D1Rs or D2Rs. The top-right panel shows the proportion of MT-projecting neurons that express either D1Rs or D2Rs. The lower-right panel shows the proportion of V4-projecting FEF neurons that express either D1Rs or D2Rs. *** denotes significance at the level of 0.001 after Bonferroni correction. Significance was determined using chi-squared tests calculated on total counts. Ns displayed on the bars. Combined $P < 10^{-16}$, MT-projecting $P < 10^{-16}$, V4-projecting $P = 5 \times 10^{-4}$. Bar heights and standard error bars are calculated from the across-animal mean proportions and the exact values are described in the main text ($N = 3$ for all comparisons).

subcortical areas, as opposed to other cortical areas. Thus, given that extrastriate projections originate in layers II-III, it may not be surprising that the disproportionate expression of D1Rs, compared with D2Rs, in the extrastriate-projecting population exceeded that of the SMI-32+ neurons. It is also possible that there is a similar distribution of SMI-32+ neurons in superficial and deep layers, which has been shown in some cortical regions (Campbell and Morrison 1989) and is suggested in our own data (Fig. 4). If SMI-32 pyramidal neurons are equiprobable in superficial and deep FEF, but a higher proportion of deep SMI-32 neurons express D2Rs compared with superficial SMI-32 neurons, this might also explain why our ratio of D1R+ to D2R+ extrastriate-projecting neurons was significantly larger than in the SMI-32+ population. It has previously been shown that the majority (~89%) of these layers II-III extrastriate-projecting neurons synapse onto pyramidal neurons in area V4 (Anderson et al. 2011). Thus, the dopaminergic modulation of FEF's influence on extrastriate visual cortex is achieved predominantly via D1Rs.

Recently, it was shown that dopamine D1Rs contribute to the influence of the FEF on activity in visual cortex (Noudoost and Moore 2011a). Specifically, it was observed that V4 neurons were more visually responsive and more selective to receptive field stimuli following local infusions of a D1R antagonist within the FEF at retinotopically corresponding sites. Manipulation of both D1R- and D2R-mediated activity was sufficient to alter saccadic choices, but only changes in D1R-mediated FEF activity altered visual responses in area V4. It was suggested that the dissimilar effects of the D1R and D2R manipulations reflect differences in the relative expression of the two receptor subtypes within superficial and deep layers of the FEF (Noudoost and Moore 2011a, 2011b; Soltani et al. 2013). In the present study, although there was much lower expression of D2Rs among the visual cortex-projecting FEF neurons, D2R expression was nonetheless present. Thus, the differential effects of D1R and D2R injections on visual cortical activity is likely attributable to other reasons. For example, the lack of observed changes in visual cortex following the D2R manipulation in the above study could reflect 1) a weaker effect of D2R and insufficient power in the small number of neurons sampled; 2) a comparatively weaker expression of D2Rs compared with D1Rs; and 3) different subpopulations of visual cortex-projecting FEF neurons. Nonetheless, the presence of D2R expression among the visual cortex-projecting FEF neurons appears consistent with other studies of the effects of prefrontal dopaminergic manipulations on behavior. For example, Puig and Miller (2012, 2015) found that injections of either D1R or D2R antagonists into PFC impair visual associative learning in monkey. These results suggest that while D1Rs appear to play a predominant role in the prefrontal control of attention and working memory, both D1 and D2 receptor subtypes may be important for visual cognition.

Several lines of evidence implicate FEF neurons in the control of visual spatial attention (Latto and Cowey 1971; Moore and Fallah 2001; Thompson et al. 2005; Monosov et al. 2008) and the visual guidance of saccadic eye movements (Schafer and Moore 2007; Noudoost and Moore 2011a). The FEF's role in attention and visually guided saccades appears to operate via its influence on visual activity within extrastriate visual cortex (Moore and Armstrong 2003; Ekstrom et al. 2008; Gregoriou et al. 2009, 2012, 2014). More recently, it was found that FEF neurons projecting to area V4 disproportionately exhibit delay activity during a memory-guided saccade task (Merrikhi et al. 2017). This observation, and the observation that manipulation of D1Rs in the FEF alters visual activity in extrastriate cortex (Noudoost and Moore 2011a), combined with the implication of prefrontal D1Rs in persistent delay-period activity (Williams and Goldman-Rakic 1995; Sawaguchi 2001; Vijayraghavan et al. 2007), suggests a mechanism whereby sustained, saccade-related signals, modulated by dopamine D1Rs, directly influence the gain of feedforward sensory signals in visual cortex (Noudoost and Moore 2011b). However, until the present study, the lack of data on the distribution of dopamine receptors within the FEF, and among visual cortex-projecting neurons, has limited the development of a circuit-specific model. Our finding that virtually all extrastriate-projecting FEF neurons express D1Rs clearly indicates a direct role of D1R-mediated modulation in the top-down control of visual cortical activity.

Supplementary Material

Supplementary material is available at *Cerebral Cortex* online.

Funding

National Institute of Health (NIH) grants: National Eye Institute (grant R01-EY014924); National Institute of Mental Health (grant T32-MH01990821).

Notes

We thank S Hyde, A. Kothari, and M. Lee for technical assistance, E. Knudsen and T. Clandinin for histology and microscopy resources, and K. Shenoy for additional animal tissue. E.-Y. Choi and A. Soltani made valuable comments on the manuscript. *Conflict of Interest*: None declared.

References

Agresti A. 2003. *Categorical data analysis. 2nd ed*. Hoboken (NJ): John Wiley & Sons

Anderson JC, Kennedy H, Martin KA. 2011. Pathways of attention: synaptic relationships of frontal eye field to V4, lateral intraparietal cortex, and area 46 in macaque monkey. *J Neurosci*. 31:10872–10881.

Arnsten AF. 2011. Catecholamine influences on dorsolateral prefrontal cortical networks. *Biol Psychiatry*. 69:e89–e99.

Arnsten AF. 2015. Stress weakens prefrontal networks: molecular insults to higher cognition. *Nat Neurosci*. 18:1376–1385.

Bastos AM, Loonis R, Kornblith S, Lundqvist M, Miller EK. 2018. Laminar recordings in frontal cortex suggest distinct layers for maintenance and control of working memory. *Proc Natl Acad Sci U S A*. 115:1117–1122.

Beaulieu JM, Gainetdinov RR. 2011. The physiology, signaling, and pharmacology of dopamine receptors. *Pharmacol Rev*. 63:182–217.

Berger B, Gaspar P, Verney C. 1991. Dopaminergic innervation of the cerebral cortex: unexpected differences between rodents and primates. *Trends Neurosci*. 14:21–27.

Bergson C, Mrzljak L, Smiley JF, Pappy M, Levenson R, Goldman-Rakic PS. 1995. Regional, cellular, and subcellular variations in the distribution of D1 and D5 dopamine receptors in primate brain. *J Neurosci*. 15:7821–7836.

Bicks LK, Koike H, Akbarian S, Morishita H. 2015. Prefrontal cortex and social cognition in mouse and man. *Front Psychol*. 6:1805.

Björklund A, Dunnett SB. 2007. Dopamine neuron systems in the brain: an update. *Trends Neurosci*. 30:194–202.

Bromberg-Martin ES, Matsumoto M, Hikosaka O. 2010. Dopamine in motivational control: rewarding, aversive, and alerting. *Neuron*. 68:815–834.

Campbell MJ, Morrison JH. 1989. Monoclonal antibody to neurofilament protein (SMI-32) labels a subpopulation of pyramidal neurons in the human and monkey neocortex. *J Comp Neurol*. 282:191–205.

Constantinidis C, Franowicz MN, Goldman-Rakic PS. 2001. Coding specificity in cortical microcircuits: a multiple-electrode analysis of primate prefrontal cortex. *J Neurosci*. 21: 3646–3655.

Condé F, Lund JS, Jacobwitz DM, Baimbridge KG, Lewis DA. 1994. Local circuit neurons immunoreactive for calretinin, calbindin D-28k or parvalbumin in monkey prefrontal cortex: distribution and morphology. *J Comp Neurol*. 34:95–116.

Conte WL, Kamishina H, Reep RL. 2009. Multiple neuroanatomical tract-tracing using fluorescent Alexa Fluor conjugates of cholera toxin subunit B in rats. *Nat Protoc*. 4:1157–1166.

Cools R, D'Esposito M. 2011. Inverted-U-shaped dopamine actions on human working memory and cognitive control. *Biol Psychiatry*. 69:e113–e125.

DeFelipe J. 1997. Types of neurons, synaptic connections and chemical characteristics of cells immunoreactive for calbindin-D28K, parvalbumin and calretinin in the neocortex. *J Chem Neuroanat*. 14:1–19.

Disney AA, Reynolds JH. 2014. Expression of m1-type muscarinic acetylcholine receptors by parvalbumin-immunoreactive neurons in the primary visual cortex: a comparative study of rat, guinea pig, ferret, macaque, and human. *J Comp Neurol*. 522:986–1003.

Dubach MF, Bowden DM. 2009. BrainInfo online 3D macaque brain atlas: a database in the shape of a brain. Chicago (IL): Society for Neuroscience Annual Meeting. Abstract No. 199.5.

Durstewitz D, Seamans JK, Sejnowski TJ. 2000. Neurocomputational models of working memory. *Nat Neurosci*. 3(Suppl):1184–1191.

Ekstrom LB, Roelfsema PR, Arsenault JT, Bonmassar G, Vanduffel W. 2008. Bottom-up dependent gating of frontal signals in early visual cortex. *Science*. 321:414–417.

Essen DC, Zeki SM. 1978. The topographic organization of rhesus monkey prestriate cortex. *J Physiol*. 277:193–226.

Fallon SJ, Smulders K, Esselink RA, van de Warrenburg BP, Bloem BR, Cools R. 2015. Differential optimal dopamine levels for set-shifting and working memory in Parkinson's disease. *Neuropsychologia*. 77:42–51.

Gao WJ, Krimer LS, Goldman-Rakic PS. 2001. Presynaptic regulation of recurrent excitation by D1 receptors in prefrontal circuits. *Proc Natl Acad Sci U S A*. 98:295–300.

García-Cabezas MA, Martínez-Sánchez P, Sánchez-González MA, Garzón M, Cavada C. 2009. Dopamine innervation in the thalamus: monkey versus rat. *Cereb Cortex*. 19:424–434.

Gaspar P, Bloch B, Le Moine C. 1995. D1 and D2 receptor gene expression in the rat frontal cortex: cellular localization in different classes of efferent neurons. *Eur J Neurosci*. 7:1050–1063.

Gattass R, Gross CG. 1981. Visual topography of striate projection zone (MT) in posterior superior temporal sulcus of the macaque. *J Neurophysiol*. 46:621–638.

Gattass R, Sousa AP, Gross CG. 1988. Visuotopic organization and extent of V3 and V4 of the macaque. *J Neurosci*. 8: 1831–1845.

Glausier JR, Khan ZU, Muly EC. 2009. Dopamine D1 and D5 receptors are localized to discrete populations of interneurons in primate prefrontal cortex. *Cerebral Cortex*. 19:1820–1834.

Goldman-Rakic PS, Lidow MS, Gallager DW. 1990. Overlap of dopaminergic, adrenergic, and serotoninergic receptors and complementarity of their subtypes in primate prefrontal cortex. *J Neurosci*. 10:2125–2138.

Gonzalez-Islas C, Hablitz JJ. 2003. Dopamine enhances EPSCs in layer II–III pyramidal neurons in rat prefrontal cortex. *J Neurosci*. 23:867–875.

González-Burgos G, Kröner S, Krimer LS, Seamans JK, Urban NN, Henze DA, Lewis DA, Barrionuevo G. 2002. Dopamine modulation of neuronal function in the monkey prefrontal cortex. *Physiol Behav*. 77:537–543.

Gregoriou GG, Gotts SJ, Desimone R. 2012. Cell-type-specific synchronization of neural activity in FEF with V4 during attention. *Neuron*. 73:581–594.

Gregoriou GG, Gotts SJ, Zhou H, Desimone R. 2009. High-frequency, long-range coupling between prefrontal and visual cortex during attention. *Science*. 324:1207–1210.

Gregoriou GG, Rossi AF, Ungerleider LG, Desimone R. 2014. Lesions of prefrontal cortex reduce attentional modulation of neuronal responses and synchrony in V4. *Nat Neurosci*. 17:1003-1011.

Gulledge AT, Jaffe DB. 1998. Dopamine decreases the excitability of layer V pyramidal cells in the rat prefrontal cortex. *J Neurosci*. 18:9139–9151.

Henze DA, González-Burgos GR, Urban NN, Lewis DA, Barrionuevo G. 2000. Dopamine increases excitability of pyramidal neurons in primate prefrontal cortex. *J Neurophysiol*. 84:2799–2809.

Higo N, Oishi T, Yamashita A, Matsuda K, Hayashi M. 2004. Cell type- and region-specific expression of neurogranin mRNA in the cerebral cortex of the macaque monkey. *Cereb Cortex*. 14:1134–1143.

Huerta MF, Krubitzer LA, Kaas JH. 1986. Frontal eye field as defined by intracortical microstimulation in squirrel monkeys, owl monkeys, and macaque monkeys: I. Subcortical connections. *J Comp Neurol*. 253:415–439.

Latto R, Cowey A. 1971. Visual field defects after frontal eye-field lesions in monkeys. *Brain Res*. 30:1–24.

Levitt P, Rakic P, Goldman-Rakic P. 1984. Region-specific distribution of catecholamine afferents in primate cerebral cortex: a fluorescence histochemical analysis. *J Comp Neurol*. 227:23–36.

Lidow MS, Goldman-Rakic PS, Gallager DW, Rakic P. 1991. Distribution of dopaminergic receptors in the primate cerebral cortex: quantitative autoradiographic analysis using [3H]raclopride, [3H]spiperone and [3H]SCH23390. *Neuroscience*. 40:657–671.

Lidow MS, Goldman-Rakic PS, Rakic P, Innis RB. 1989. Dopamine D2 receptors in the cerebral cortex: distribution and pharmacological characterization with [3H]raclopride. *Proc Natl Acad Sci U S A*. 86:6412–6416.

Melchitzky DS, Sesack SR, Lewis DA. 1999. Parvalbumin-immunoreactive axon terminals in macaque monkey and human prefrontal cortex: laminar, regional, and target specificity of type I and type II synapses. *J Comp Neurol*. 408:11–22.

Merrikhi Y, Clark K, Albarran E, Parsa M, Zirnsak M, Moore T, Noudoost B. 2017. Spatial working memory alters the efficacy of input to visual cortex. *Nat Commun*. 8:15041.

Missale C, Nash SR, Robinson SW, Jaber M, Caron MG. 1998. Dopamine receptors: from structure to function. *Physiol Rev*. 78:189–225.

Monosov IE, Trageser JC, Thompson KG. 2008. Measurements of simultaneously recorded spiking activity and local field potentials suggest that spatial selection emerges in the frontal eye field. *Neuron*. 57:614–625.

Moore T, Armstrong KM. 2003. Selective gating of visual signals by microstimulation of frontal cortex. *Nature*. 421:370–373.

Moore T, Fallah M. 2001. Control of eye movements and spatial attention. *Proc Natl Acad Sci U S A*. 98:1273–1276.

Moschovakis AK, Gregoriou GG, Ugolini G, Doldan M, Graf W, Guldin W, Hadjidimitrakis K, Savaki HE. 2004. Oculomotor areas of the primate frontal lobes: a transneuronal transfer of rabies virus and [14C]-2-deoxyglucose functional imaging study. *J Neurosci*. 24:5726–5740.

Mueller A, Hong DS, Shepard S, Moore T. 2017. Linking ADHD to the neural circuitry of attention. *Trends Cogn Sci*. 21:474–488.

Mueller A, Shepard SB, Moore T. 2018. Differential expression of dopamine D5 receptors across neuronal subtypes in macaque frontal eye field. *Front Neural Circuits*. 12:12.

Muly EC, Szigeti K, Goldman-Rakic PS. 1998. D1 receptor in interneurons of macaque prefrontal cortex: distribution and subcellular localization. *J Neurosci*. 18:10553–10565.

Noriega NC, Garyfallou VT, Kohama SG, Urbanski HF. 2007. Glutamate receptor subunit expression in the rhesus macaque locus coeruleus. *Brain Res*. 1173:53–65.

Noudoost B, Moore T. 2011a. Control of visual cortical signals by prefrontal dopamine. *Nature*. 474:372–375.

Noudoost B, Moore T. 2011b. The role of neuromodulators in selective attention. *Trends Cogn Sci*. 15:585–591.

Ott T, Jacob SN, Nieder A. 2014. Dopamine receptors differentially enhance rule coding in primate prefrontal cortex neurons. *Neuron*. 84:1317–1328.

Parthasarathy HB, Schall JD, Graybiel AM. 1992. Distributed but convergent ordering of corticostriatal projections: analysis of the frontal eye field and the supplementary eye field in the macaque monkey. *J Neurosci*. 12:4468–4488.

Percheron G, François C, Pouget P. 2015. What makes a frontal area of primate brain the frontal eye field? *Front Integr Neurosci*. 9:33.

Puig MV, Miller EK. 2012. The role of prefrontal dopamine D1 receptors in the neural mechanisms of associative learning. *Neuron*. 74:874–886.

Puig MV, Miller EK. 2015. Neural substrates of dopamine D2 receptor modulated executive functions in the monkey prefrontal cortex. *Cereb Cortex*. 25:2980–2987.

Rohlfing T, Kroenke CD, Sullivan EV, Dubach MF, Bowden DM, Grant KA, Pfefferbaum A. 2012. The INIA19 template and NeuroMaps atlas for primate brain image parcellation and spatial normalization. *Front Neuroinform*. 6:27.

Saleem KS, Logothetis NK. 2012. *A combined MRI and histology atlas of the rhesus monkey brain in stereotaxic coordinates*. San Diego (CA): Elsevier Science Publishing Co Inc

Santana N, Artigas F. 2017. Laminar and cellular distribution of monoamine receptors in rat medial prefrontal cortex. *Front Neuroanat*. 11:87.

Santana N, Mengod G, Artigas F. 2009. Quantitative analysis of the expression of dopamine D1 and D2 receptors in pyramidal and GABAergic neurons of the rat prefrontal cortex. *Cereb Cortex*. 19:849–860.

Sawaguchi T. 2001. The effects of dopamine and its antagonists on directional delay-period activity of prefrontal neurons in monkeys during an oculomotor delayed-response task. *Neurosci Res*. 41:115–128.

Sawaguchi T, Goldman-Rakic PS. 1991. D1 dopamine receptors in prefrontal cortex: involvement in working memory. *Science*. 251:947–950.

Sawaguchi T, Goldman-Rakic PS. 1994. The role of D1-dopamine receptor in working memory: local injections of dopamine antagonists into the prefrontal cortex of rhesus monkeys performing an oculomotor delayed-response task. *J Neurophysiol*. 71:515–528.

Schafer RJ, Moore T. 2007. Attention governs action in the primate frontal eye field. *Neuron*. 56:541–551.

Schall JD, Morel A, King DJ, Bullier J. 1995. Topography of visual cortex connections with frontal eye field in macaque: convergence and segregation of processing streams. *J Neurosci*. 15:4464–4487.

Schnell SA, Staines WA, Wessendorf MW. 1999. Reduction of lipofuscin-like autofluorescence in fluorescently labeled tissue. *J Histochem Cytochem*. 47:719–730.

Schnyder H, Reisine H, Hepp K, Henn V. 1985. Frontal eye field projection to the paramedian pontine reticular formation traced with wheat germ agglutinin in the monkey. *Brain Res*. 329:151–160.

Seamans JK, Gorelova N, Durstewitz D, Yang CR. 2001. Bidirectional dopamine modulation of GABAergic inhibition in prefrontal cortical pyramidal neurons. *J Neurosci*. 21:3628–3638.

Seamans JK, Yang CR. 2004. The principal features and mechanisms of dopamine modulation in the prefrontal cortex. *Prog Neurobiol*. 74:1–58.

Senzai Y, Fernandez-Ruiz A, Buzsáki G. 2019. Layer-specific physiological features and interlaminar interactions in the primary visual cortex of the mouse. *Neuron*. 101:1–14.

Singec I, Knoth R, Ditter M, Volk B, Frotscher M. 2004. Neurogranin is expressed by principal cells but not interneurons in the rodent and monkey neocortex and hippocampus. *J Comp Neurol*. 479:30–42.

Smiley JF, Levey AI, Ciliax BJ, Goldman-Rakic PS. 1994. D1 dopamine receptor immunoreactivity in human and monkey cerebral cortex: predominant and extrasynaptic localization in dendritic spines. *Proc Natl Acad Sci U S A*. 91:5720–5724.

Soltani A, Noudoost B, Moore T. 2013. Dissociable dopaminergic control of saccadic target selection and its implications for reward modulation. *Proc Natl Acad Sci U S A*. 110: 3579–3584.

Squire RF, Noudoost B, Schafer RJ, Moore T. 2013. Prefrontal contributions to visual selective attention. *Annu Rev Neurosci*. 36:451–466.

Stanton GB, Bruce CJ, Goldberg ME. 1995. Topography of projections to posterior cortical areas from the macaque frontal eye fields. *J Comp Neurol*. 353:291–305.

Thompson KG, Biscoe KL, Sato TR. 2005. Neuronal basis of covert spatial attention in the frontal eye field. *J Neurosci*. 25:9479–9487.

Tseng KY, O'Donnell P. 2004. Dopamine–glutamate interactions controlling prefrontal cortical pyramidal cell excitability involve multiple signaling mechanisms. *J Neurosci*. 24:5131–5139.

Tseng KY, O'Donnell P. 2007. D2 dopamine receptors recruit a GABA component for their attenuation of excitatory synaptic transmission in the adult rat prefrontal cortex. *Synapse*. 61:843–850.

Tsutsui KI, Oyama K, Nakamura S, Iijima T. 2016. Comparative overview of visuospatial working memory in monkeys and rats. *Front Syst Neurosci*. 10:99.

Ungerleider LG, Galkin TW, Desimone R, Gattass R. 2008. Cortical connections of area V4 in the macaque. *Cereb Cortex*. 18:477–499.

Uylings HB, Groenewegen HJ, Kolb B. 2003. Do rats have a prefrontal cortex? *Behav Brain Res*. 146:3–17.

Vijayraghavan S, Wang M, Birnbaum SG, Williams GV, Arnsten AF. 2007. Inverted-U dopamine D1 receptor actions on prefrontal neurons engaged in working memory. *Nat Neurosci*. 10:376–384.

Vijayraghavan S, Major AJ, Everling S. 2016. Dopamine D1 and D2 receptors make dissociable contributions to dorsolateral prefrontal cortical regulation of rule-guided oculomotor behavior. *Cell Rep*. 16:805–816.

Vincent SL, Khan Y, Benes FM. 1993. Cellular distribution of dopamine D1 and D2 receptors in rat medial prefrontal cortex. *J Neurosci*. 13:2551–2564.

Voelker CC, Garin N, Taylor JS, Gähwiler BH, Hornung JP, Molnár Z. 2004. Selective neurofilament (SMI-32, FNP-7 and N200) expression in subpopulations of layer V pyramidal neurons in vivo and in vitro. *Cereb Cortex*. 14: 1276–1286.

Wang J, O'Donnell P. 2001. D(1) dopamine receptors potentiate nmda-mediated excitability increase in layer V prefrontal cortical pyramidal neurons. *Cereb Cortex*. 11:452–462.

Wang XJ, Tegnér J, Constantinidis C, Goldman-Rakic PS. 2004a. Division of labor among distinct subtypes of inhibitory neurons in a cortical microcircuit of working memory. *Proc Natl Acad Sci U S A*. 101: 1368–1373.

Wang Y, Vijayraghavan S, Goldman-Rakic PS. 2004b. Selective D2 receptor actions on the functional circuitry of working memory. *Science*. 303:853–856.

Watanabe M, Kodama T, Hikosaka K. 1997. Increase of extracellular dopamine in primate prefrontal cortex during a working memory task. *J Neurophysiol*. 78:2795–2798.

Wei X, Ma T, Cheng Y, Huang CCY, Wang X, Lu J, Wang J. 2017. Dopamine D1 or D2 receptor-expressing neurons in the central nervous system. *Addict Biol*. 23:569-584.

Williams GV, Goldman-Rakic PS. 1995. Modulation of memory fields by dopamine D1 receptors in prefrontal cortex. *Nature*. 376:572–575.

Williams SM, Goldman-Rakic PS. 1998. Widespread origin of the primate mesofrontal dopamine system. *Cereb Cortex*. 8:321–345.

Williams SM, Goldman-Rakic PS, Leranth C. 1992. The synaptology of parvalbumin-immunoreactive neurons in the primate prefrontal cortex. *J Comp Neurol*. 320:353–369.

Xu L, Tanigawa H, Fujita I. 2003. Distribution of alpha-amino-3-hydroxy-5-methyl-4-isoxazolepropionate-type glutamate receptor subunits (GluR2/3) along the ventral visual pathway in the monkey. *J Comp Neurol*. 456:396–407.

Zheng P, Zhang XX, Bunney BS, Shi WX. 1999. Opposite modulation of cortical N-methyl-D-aspartate receptor-mediated responses by low and high concentrations of dopamine. *Neuroscience*. 91:527–535.